AD-A108 755 NAVAL UNDERWATER SYSTEMS CENTER NEW LONDON CT NEW LO--ETC F/6 20/1
FRAM II SINGLE CHANNEL AMBIENT NOISE STATISTICS: A PAPER PRESEN--ETC(U)
NOV 81 R F DWYER
UNCLASSIFIED NUSC/TD-6583 NL

END
DATE
FILMED
1 82
DTIC

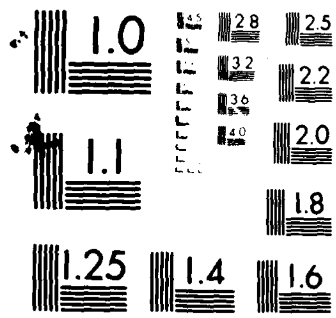

MICROCOPY RESOLUTION TEST CHART
NATIONAL BUREAU OF STANDARDS 1963-A

NUSC Technical Document 6583
25 November 1981

(12) LEVEL

FRAM II
Single Channel
Ambient Noise Statistics

A Paper Presented at the 101st Meeting of the Acoustical Society of America, 19 May 1981, Ottawa, Canada

Roger F. Dwyer
Surface Ship Sonar Department

Naval Underwater Systems Center
Newport, Rhode Island / New London, Connecticut

Preface

This technical document was prepared under project No. A75028, "Adaptive Nonparametric Sequential Detection," Principal Investigator, R. F. Dwyer (Code 333); Program Element 61152N, Navy Subproject/Task ZR0000101, "In-House Laboratory Independent Research," Program Manager, J. Parrish (MAT 08L).

The author appreciates and acknowledges the many contributions of F. R. DiNapoli (Arctic Program Manager) and E. H. Hug (NUSC Scientific Staff) to this study on arctic ambient noise.

Reviewed and Approved: 25 November 1981

W. A. Von Winkle

W. A. Von Winkle
Associate Technical Director
for Technology

The author of this document is located at the New London Laboratory, Naval Underwater Systems Center, New London, Connecticut 06320.

REPORT DOCUMENTATION PAGE		READ INSTRUCTIONS BEFORE COMPLETING FORM
1. REPORT NUMBER TD 6583	2. GOVT ACCESSION NO. AD-A108 755	3. RECIPIENT'S CATALOG NUMBER
4. TITLE (and Subtitle) FRAM II SINGLE CHANNEL AMBIENT NOISE STATISTICS A PAPER PRESENTED AT THE 101ST MEETING OF THE ACOUSTICAL SOCIETY OF AMERICA, 19 MAY 1981, OTTAWA, CANADA		5. TYPE OF REPORT & PERIOD COVERED 6. PERFORMING ORG. REPORT NUMBER
7. AUTHOR(s) Roger F. Dwyer		8. CONTRACT OR GRANT NUMBER(s)
9. PERFORMING ORGANIZATION NAME AND ADDRESS Naval Underwater Systems Center New London Laboratory New London, CT 06320		10. PROGRAM ELEMENT, PROJECT, TASK AREA & WORK UNIT NUMBERS A75030
11. CONTROLLING OFFICE NAME AND ADDRESS Naval Material Command (MAT 08L) Washington, DC 20360		12. REPORT DATE 25 November 1981 13. NUMBER OF PAGES 30
14. MONITORING AGENCY NAME & ADDRESS (if different from Controlling Office)		15. SECURITY CLASS. (of this report) UNCLASSIFIED 15a. DECLASSIFICATION/DOWNGRADING SCHEDULE

16. DISTRIBUTION STATEMENT (of this Report)

Approved for public release; distribution unlimited.

17. DISTRIBUTION STATEMENT (of the abstract entered in Block 20, if different from Report)

18. SUPPLEMENTARY NOTES

19. KEY WORDS (Continue on reverse side if necessary and identify by block number)

Arctic Ambient Noise
Non-Gaussiar Noise

20. ABSTRACT (Continue on reverse side if necessary and identify by block number)

This document contains the oral and visual presentation given at the 101st Meeting of the Acoustical Society of America, 19 May 1981, Ottawa, Canada.

This document describes the results of a statistical analysis study of FRAM II arctic under-ice ambient noise data. The specific data that were analyzed were recorded on 23-24 April 1980 from a pack ice camp in the Arctic Ocean, located at 86°N latitude, 25°W longitude. At this location, the bottom

DD FORM 1 JAN 73 1473

20. (Continued)

depth was approximately 4000 m. The measurement system consisted of a broadband omnidirectional hydrophone, suspended to a depth of 91 m from a sonobuoy located in a lead. Under the influence of arctic currents, the pack ice was slowly moving. This movement caused rifting and cracking of ice, which occurred, at times, throughout the experiments and represented a structured acoustic noise source. Both impulsive and burst noise were identified in the data and were probably created by tensile cracks and rubbing ice masses.

In order to better understand the statistical properties of under-ice ambient noise, the skew, kurtosis, and cumulative distribution function (cdf) of the data were estimated. In the time domain, the statistics were estimated in 100, 350, and 2500 Hz bands. At times, the statistical estimates in all bands deviated from Gaussian noise significantly, and were consistent with previously reported results of experiments made within the Canadian Arctic Archipelago. The estimated energy cdf of FRAM II data predicted detection thresholds 3 to 10 dB higher than what would be expected from purely Gaussian phenomena. Spectrum levels and spectrograms were also measured. The spectrograms depicted dynamic frequency components that appear, from aural information that sounded like squeaks, to be correlated with ice dynamics. Comparisons of broadband spectrum level estimates at different times indicate non-stationary frequency domain components that also appear to be correlated with ice dynamics.

Since it was known that burst noise durations of arctic under-ice noise have been measured to last from 0.1 to 1/3 second, statistical estimates of frequency domain components were measured. These frequency domain statistical measurements represent new techniques for estimated environmental noise phenomena. The complex skew, kurtosis, and cdf were measured in 1, 2, 6, and 10 Hz resolution cells at the output of a discrete Fourier transform with processing times from 2 to 14 minutes. These new findings indicate the existence of strong non-Gaussian noise in the frequency domain.

Fram II Single Channel Ambient Noise Statistics

Introduction

This presentation discusses the results of a statistical data analysis study of under-ice ambient noise. The data were obtained from a multi-institutional Arctic Ocean experiment conducted in the spring of 1980.

The author's motivations for analyzing under-ice ambient noise were due to his interest in non-Gaussian noise processing techniques and to the published experimental results of A. R. Milne and others in which they concluded that under-ice ambient noise in the time domain was at times impulsive and highly non-Gaussian. In the course of our analyses, we repeated Milne's experimental measurements (albeit with different bandwidths) and deduced similar conclusions on the non-Gaussian nature in the time domain of under-ice ambient noise. By statistically examining the discrete frequency components, we found that they were also non-Gaussian due to ice dynamics. These new findings indicate the existence of strong non-Gaussian noise in the frequency domain.

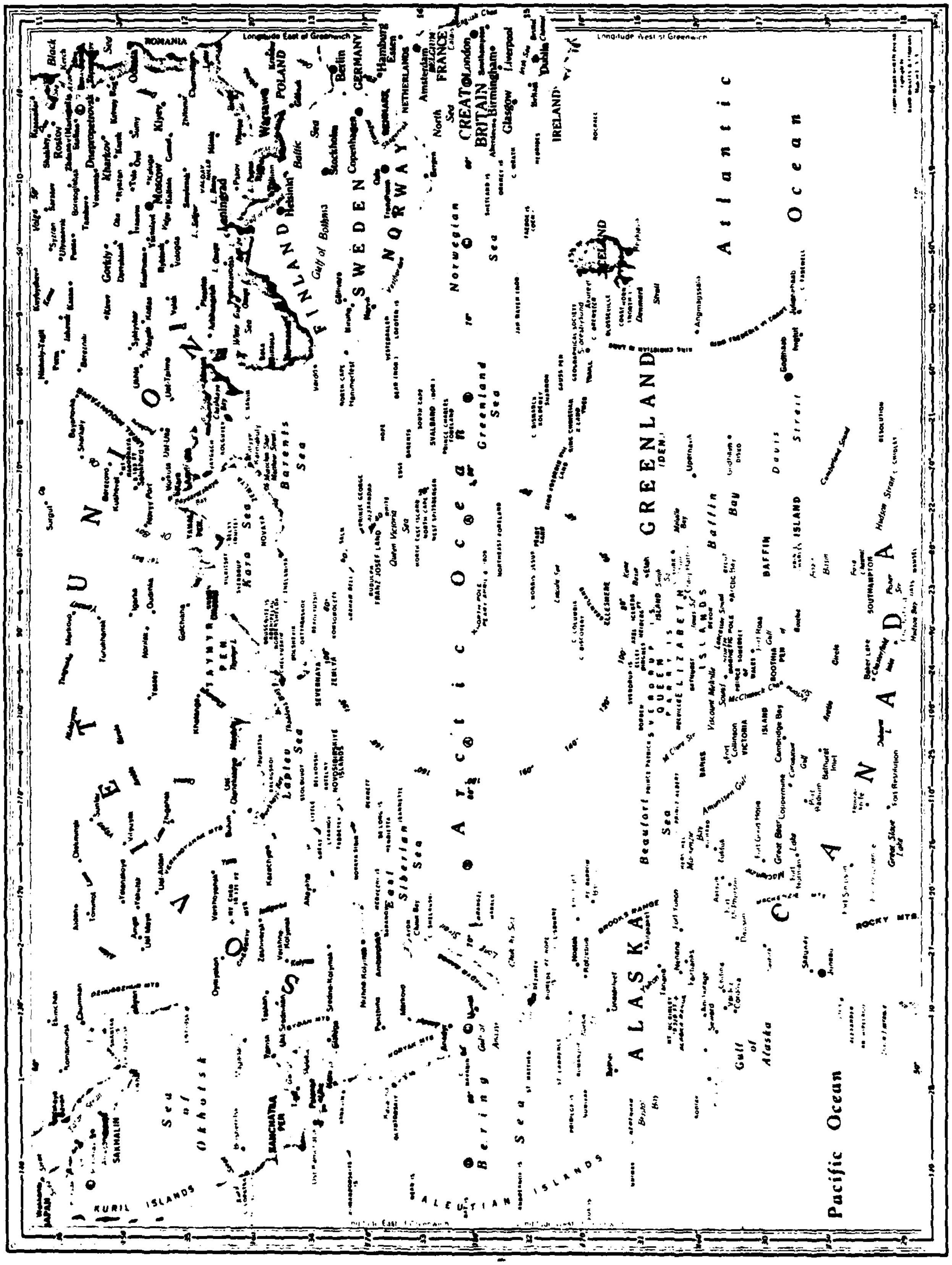
Arctic Ocean
Atlantic Ocean
Pacific Ocean
GREENLAND
ALASKA
CANADA
SWEDEN
NORWAY
FINLAND
IRELAND
GREAT BRITAIN
Barents Sea
Greenland Sea
Norwegian Sea
Bering Sea
Sea of Okhotsk
Beaufort Sea
Baffin Bay
Davis Strait
KURIL ISLANDS
ALEUTIAN ISLANDS
Gulf of Alaska

Slide 1

The specific data that have been analyzed were recorded on 23-24 April 1980 at location 86° N latitude, 25° W longitude by scientists from MIT, WOI, NUSC, and from other institutions in the United States and Canada. The group conducting the experiments were camped on pack ice that was slowly moving under the influence of arctic currents, wind, and neighboring floes.

The data collected by A. R. Milne and others were obtained in the Canadian Archipeligo region under stationary shore fast ice. In this region, the mechanism for impulsive and non-Gaussian noise is due to tensile stresses caused by rapid reduction in air temperatures. Noise from the pack ice, on the other hand, is due to the friction between interacting and colliding ice floes in addition to tensile stresses.

Camp Site

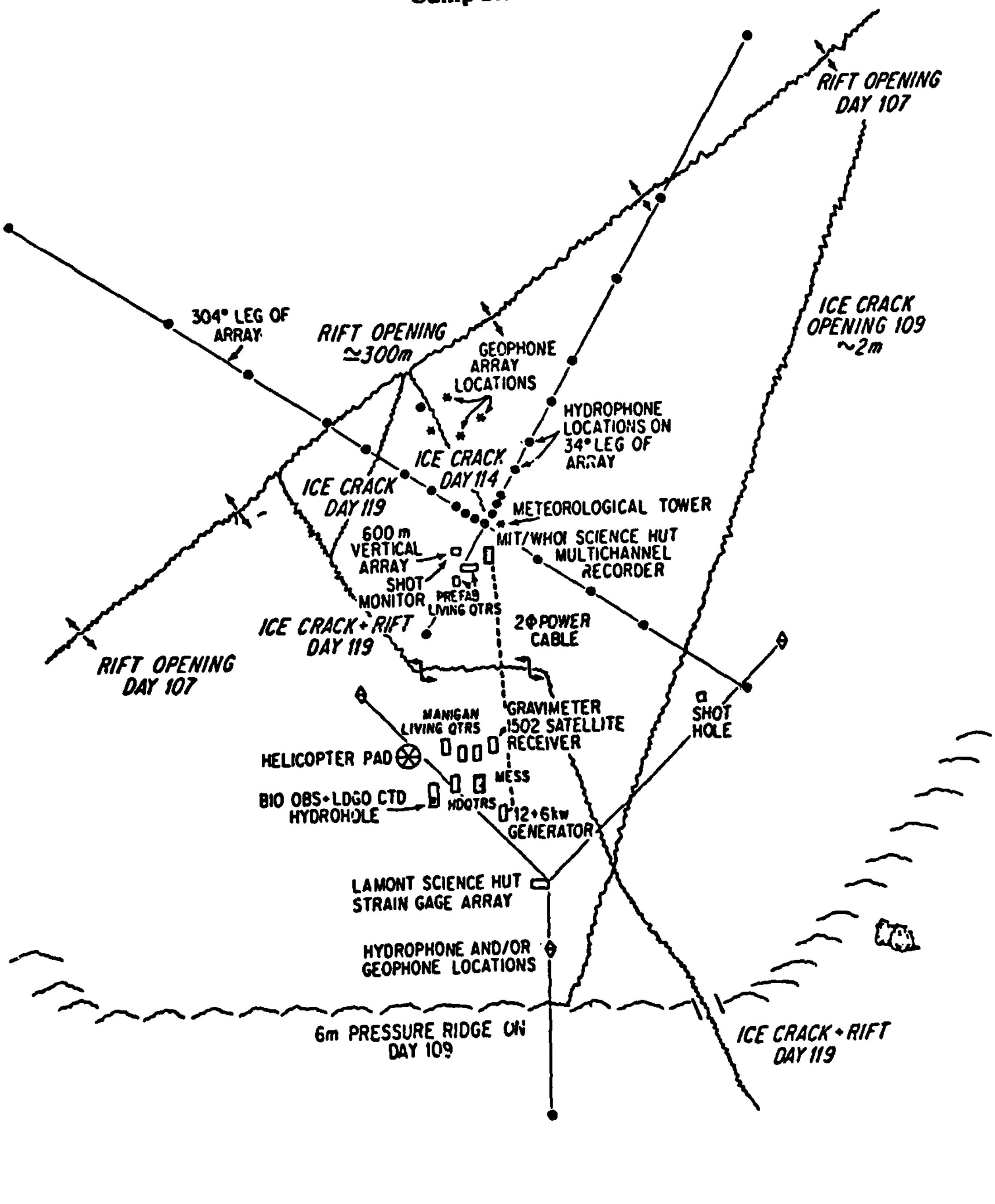
RIFT OPENING
DAY 107
304° LEG OF
ARRAY
RIFT OPENING
≃300m
GEOPHONE
ARRAY
LOCATIONS
ICE CRACK
OPENING 109
~2m
HYDROPHONE
LOCATIONS ON
34° LEG OF
ARRAY
ICE CRACK
DAY 114
ICE CRACK
DAY 119
METEOROLOGICAL TOWER
600 m
VERTICAL
ARRAY
MIT/WHOI SCIENCE HUT
MULTICHANNEL
RECORDER
SHOT
MONITOR
PREFAB
LIVING QTRS
ICE CRACK + RIFT
DAY 119
2Φ POWER
CABLE
RIFT OPENING
DAY 107
MANIGAN
LIVING QTRS
GRAVIMETER
1502 SATELLITE
RECEIVER
SHOT
HOLE
HELICOPTER PAD
MESS
BIO OBS+LDGO CTD
HYDROHOLE
HDQTRS
12+6kw
GENERATOR
LAMONT SCIENCE HUT
STRAIN GAGE ARRAY
HYDROPHONE AND/OR
GEOPHONE LOCATIONS
6m PRESSURE RIDGE ON
DAY 109
ICE CRACK + RIFT
DAY 119

Slide 2

The camp site, as shown in this slide (from an MIT cruise report), was plagued by rifts and ice crack openings while the scientific experiments were being conducted.

The data of this presentation are from a sonobuoy located in a lead near the large low frequency array. An omnidirectional hydrophone was suspended from the sonobuoy to a depth of 91 m below the ice. The original recording bandwidth was from 10 Hz to 5 kHz. However, our recording bandwidth only extended from 10 to 2.5 kHz. The water depth, which is an important parameter for predicting propagation conditions, was approximately 4000 m in this location.

Non-Stationary Under-Ice Ambient Noise

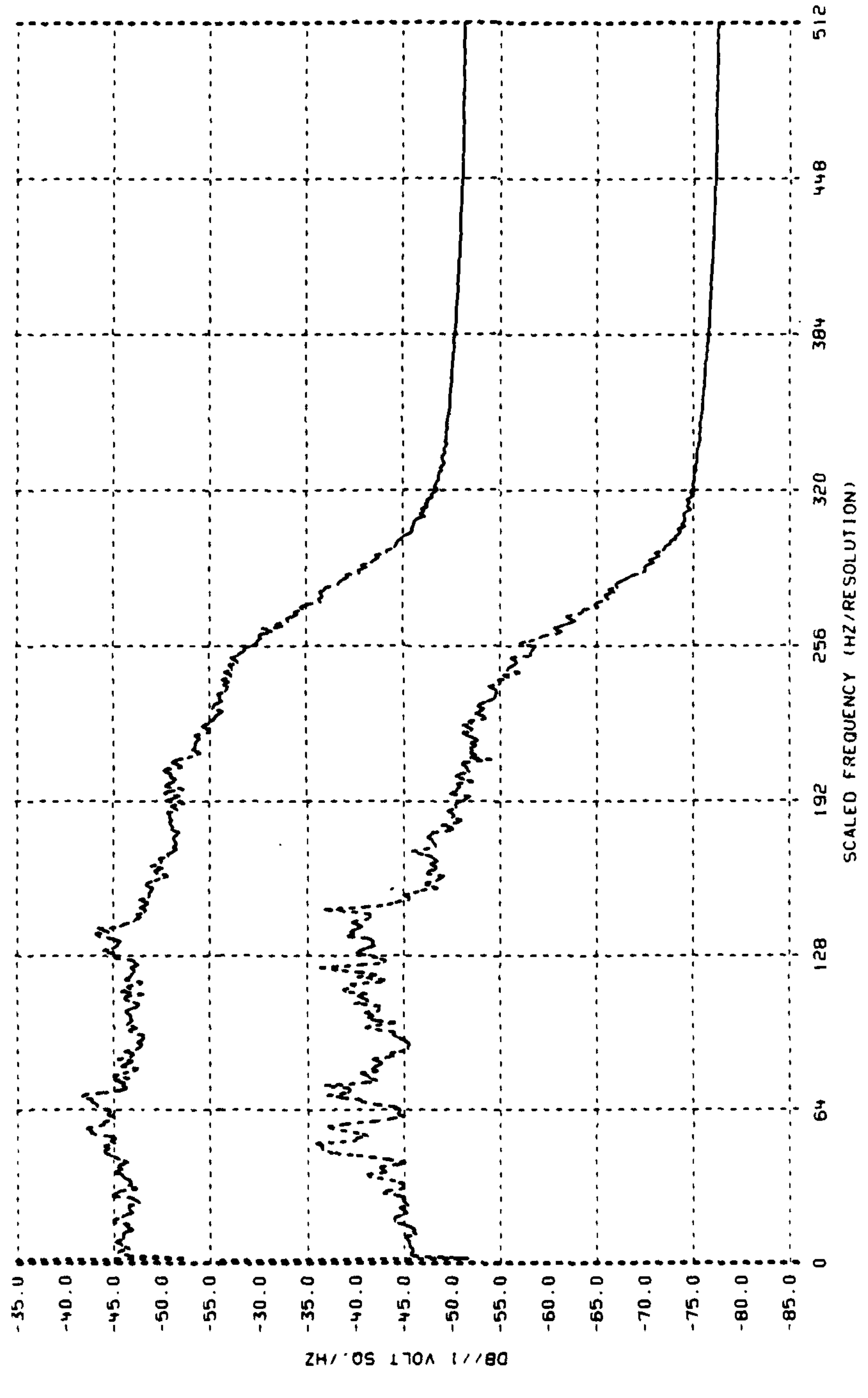

Slide 3

After digitizing the data at a 10-kHz rate, we compared its spectrum for 2 time periods. The top curve represents the average spectrum using 100 consecutive 1024 point FFT estimates, which is equivalent to about 10 seconds of data. The same procedure was utilized for the bottom curve except that the estimates were made 3 minutes later. The horizontal scale is given in terms of the normalized frequency. Multiply by 10 to convert to approximate frequency.

Statistical Moments

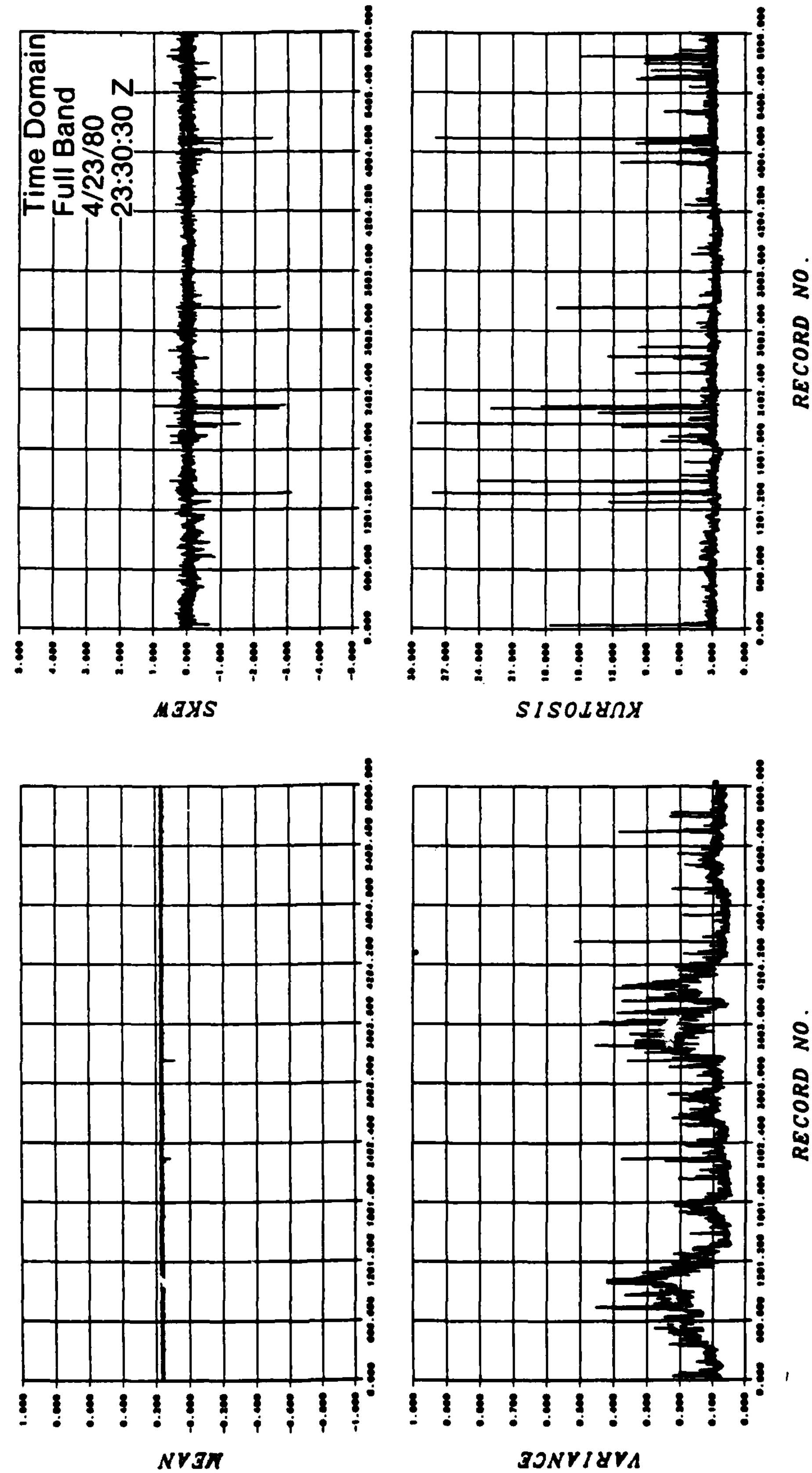

Slide 4

The first four statistical moments, in the time domair, of the data are given here. They were estimated in 1024 sample blocks, which we identify as records in each of the four figures on the horizontal axes. Since the sampling rate was 10 kHz, each record represents about 0.1 second of time. The total 6006 records, therefore, represent 10 minutes of data.

The graph on the top left shows that the mean of the data is not zero. This bias was due to the carrier frequency of the tape recorder being slightly misaligned. In subsequent processing we subtracted out this bias.

The next graph on the bottom left shows the variance of the data. Note the large variability of the variance over time. In order to assess which frequencies were dominating the variance in the full band, we process the data in smaller frequency bandwidths. These bands were from 100-200 Hz, 200-300 Hz, 300-400 Hz, 400-750 Hz, 750-1100 Hz, and 1100-1450 Hz. The 300-400 Hz band will be shown in a later slide. We found that the higher frequency bands (i.e., 750-1100 Hz and 1100-1450 Hz) were responsible for variability in the variance.

The top right graph represents the estimated skew. It is defined as the third central moment divided by the cube of the standard deviation. The skew measures the symmetry of the data compared with a Gaussian distribution. For a Gaussian process the skew is zero, within confidence bounds determined by the number of samples used in the estimate. We can see from this graph that some records deviate from the Gaussian assumption based on the skew by a large factor.

The last graph on the bottom right shows the kurtosis. It is defined as the fourth central moment divided by the square of the variance. The kurtosis measures the peakedness of the data compared with a Gaussian distribution. For a Gaussian process, the kurtosis is 3, within a confidence bound determined by the number of samples used in the estimate. As shown here, many records deviate from the Gaussian assumption based on the kurtosis.

In the next slide, we will show the estimated cumulative distribution function of the data for two cases. The first, 300 records (approximately 300,000 samples) was utilized for our estimate for case one, and the second, a 300 record length, starting at about the 1800th record, was used.

TIME DOMAIN: ENERGY DISTRIBUTION

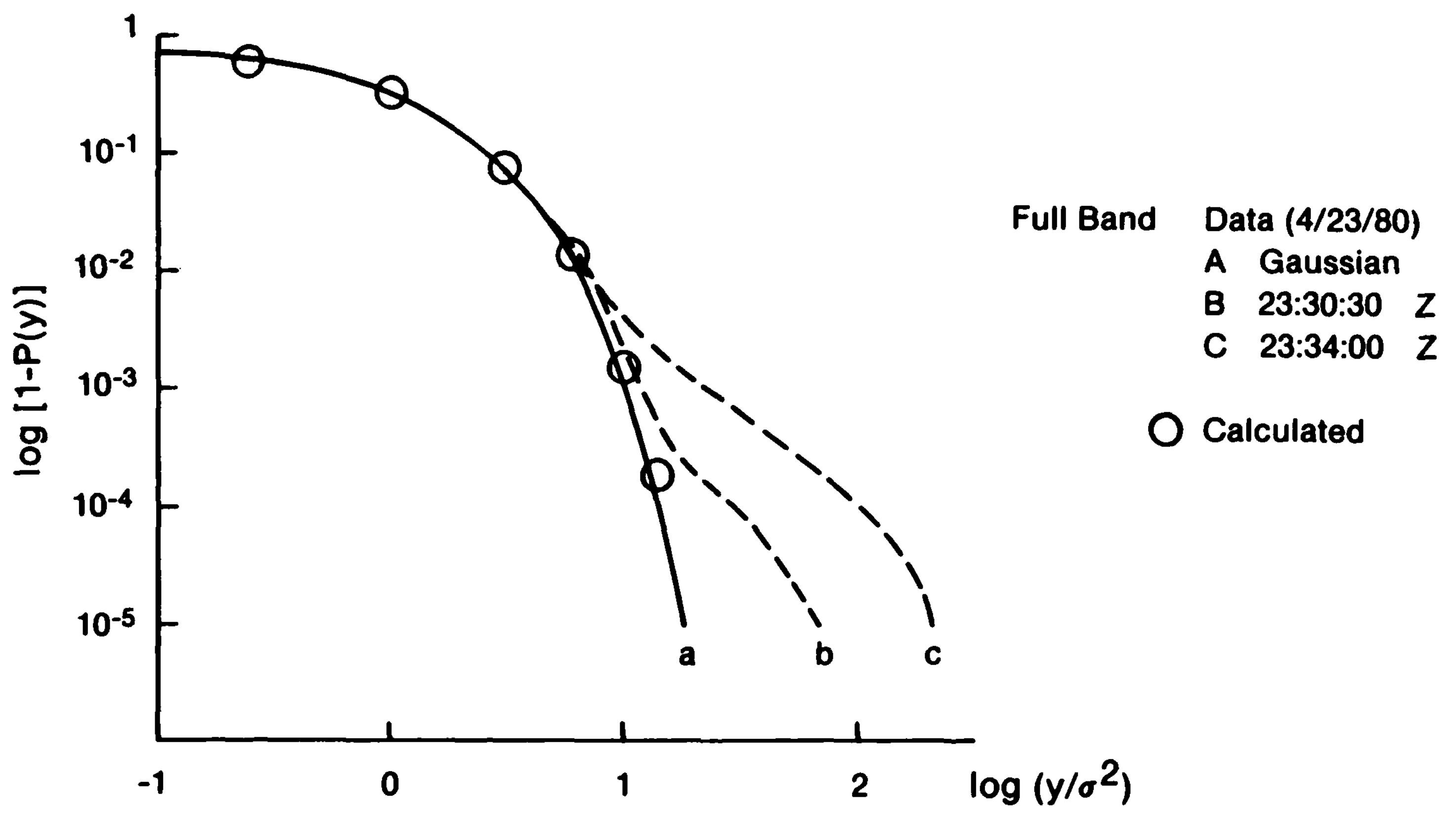

Slide 5

The estimated time domain energy distribution is shown here. Each sample was first squared and then the cumulative distribution function (cdf) was estimated for the 300 records, which represents a time interval of about 30 seconds. The vertical axis is plotted as the logarithm of the excedance probability. The squared data are normalized by dividing the output by the input variance, and then, as shown, the horizontal axis is plotted as the logarithm of the normalized output.

The solid curve represents the cdf of a known Gaussian noise source that was digitized and processed exactly as the data. The circles are analytical calculations for the energy cdf assuming a Gaussian input. The curves b and c represent the data for the first and second 300 records, respectively. The significance of these plots can be appreciated by a simple example.

Suppose we want to set a threshold in an energy detector so that the false alarm rate is 0.0001. From the graph, we would have to set the threshold 3-4 dB higher for curve b, and 9-10 dB higher for curve c, compared with what the threshold would be set at for purely Gaussian noise.

Frequency Domain
Time
10 sec
4/23/80
23:30:45
0.2
1.0
1.8
Frequency (kHz)

Slide 6

To understand the frequency domain aspects of the under-ice ambient noise, we processed the data spectrum in a frequency-time format. The vertical axis represents time. The total time in this graph is about 2.5 minutes. The horizontal axis is frequency extended out to 2 kHz. We processed the data spectrum with a resolution of 2 Hz.

From the slide, we can see large but dynamic tonals in the data occurring over this time interval. These events sounded like squeaks and appear to be due to ice dynamics.

Statistics in the Frequency Domain

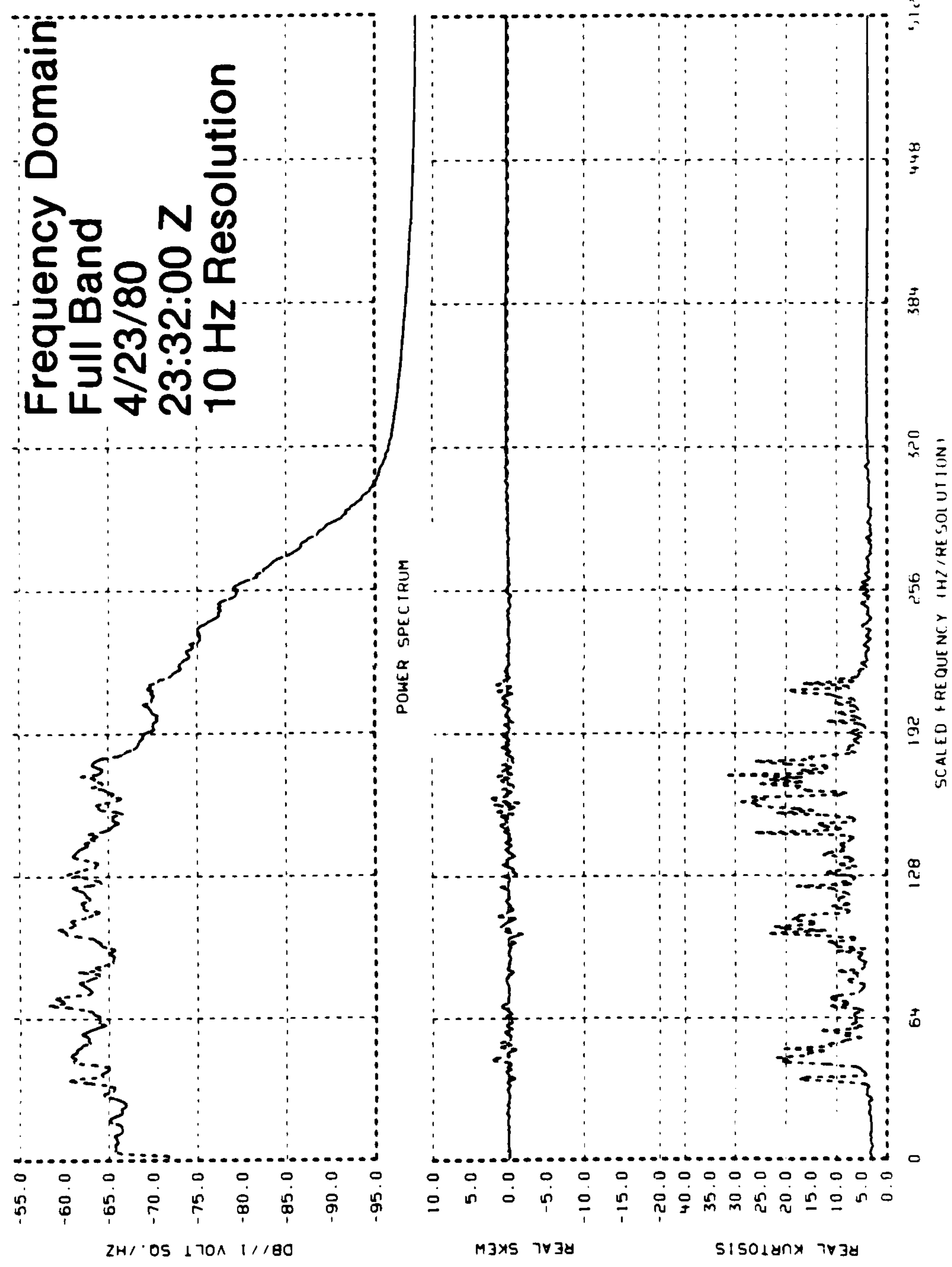

Slide 7

An important aspect of our study of under-ice ambient noise was an evaluation of the statistics in the frequency domain. Usually, the statistics of acoustic noise in the frequency domain are assumed Gaussian. As we shall show, this is not necessarily the case in the Arctic. These results are new and are presented here apparently for the first time.

For the full band case with a sampling rate of 10 kHz and utilizing a 1024 point FFT, we obtained an average power spectrum with a 10 Hz resolution for 1000 consecutive FFT's. The total time for the estimate was 1.7 minutes. For the 1000 consecutive FFT outputs, we estimated the skew and kurtosis for each bin for both the real and imaginary parts. These results are shown in the slide. The top curve represents the average power spectrum and the middle and lower curves represent the corresponding estimates of the skew and kurtosis. Only the real part is shown. Similar, but not identical, results were obtained for the imaginary part. We can see that over a wide bandwidth, many bins deviate from the Gaussian assumption based on the skew and kurtosis. However, the results are more dramatic for the kurtosis estimates. Note that the lower frequencies (i.e., below approximately 300 Hz) appear to be Gaussian. Data at other time periods show low frequency components also deviating from the Gaussian assumption based on the skew and kurtosis.

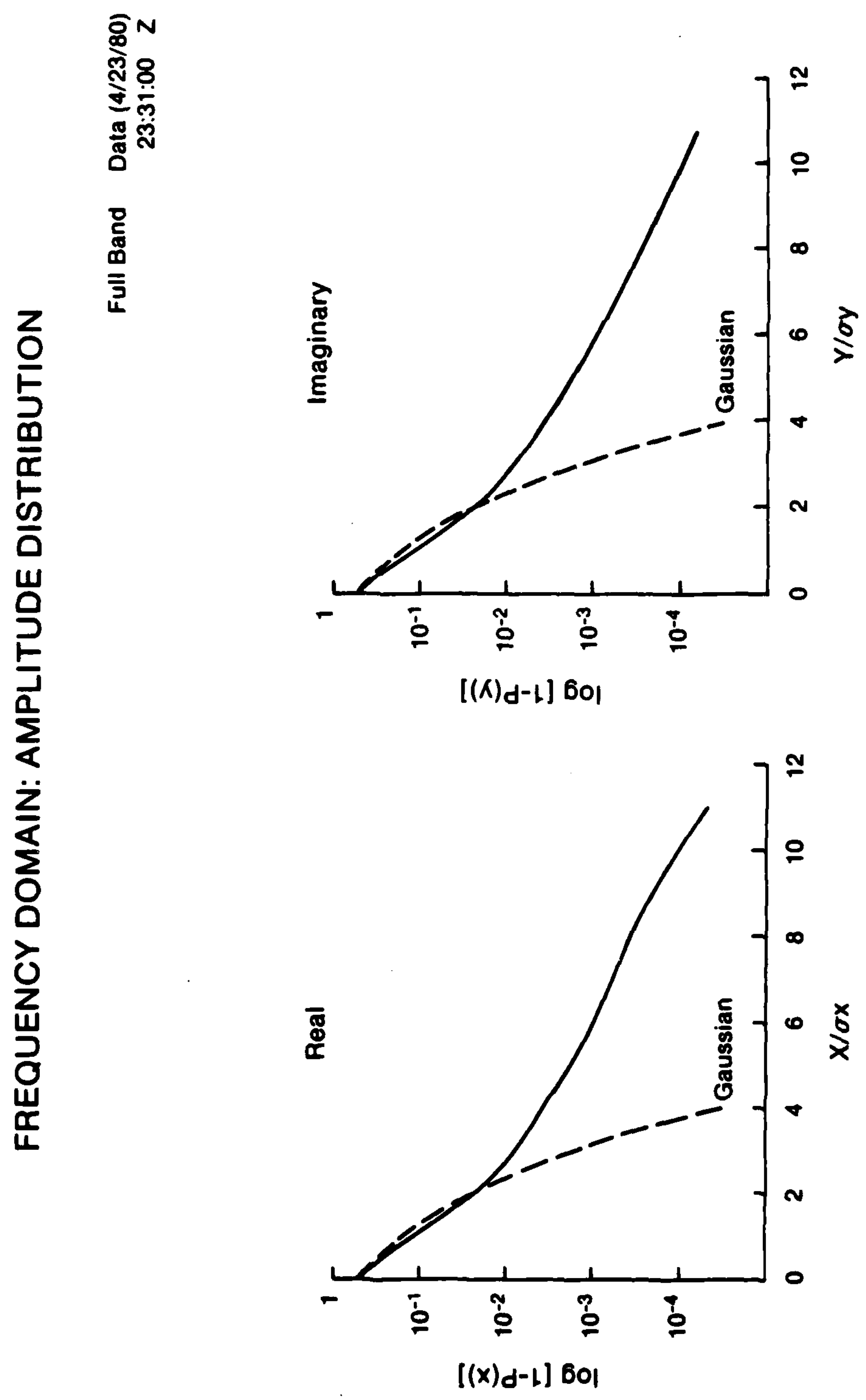
FREQUENCY DOMAIN: AMPLITUDE DISTRIBUTION
Full Band
Data (4/23/80)
23:31:00 Z
Real
Imaginary
Gaussian
Gaussian
log [1-P(x)]
log [1-P(y)]
1
10-1
10-2
10-3
10-4
0
2
4
6
8
10
12
X/σx
Y/σy

Slide 8

For the 1000 consecutive FFT outputs, we estimated the amplitude cdf over a relative flat portion of the band for both the real and imaginary parts. The total estimates over 1.7 minutes consisted of approximately 200,000 bins for each part.

The slide indicates the results of the amplitude cdf estimates for the real and imaginary parts. The vertical axis represents the logarithm of the excedance probability. We have normalized each amplitude by dividing by its corresponding standard deviation as shown on the horizontal axis. Also shown on each graph (indicated by the dashed curve) is the result for a Gaussian noise source that has been processed in exactly the same manner as the data. The results clearly show the significant deviation of the tests from the Gaussian distribution in the frequency domain. The data should be considered representative of the class of non-Gaussian distribution encountered in the Arctic. We have also processed other data in 6 Hz and 2 Hz resolution with similar results. The results for the 2 Hz case will be presented later in the discussion.

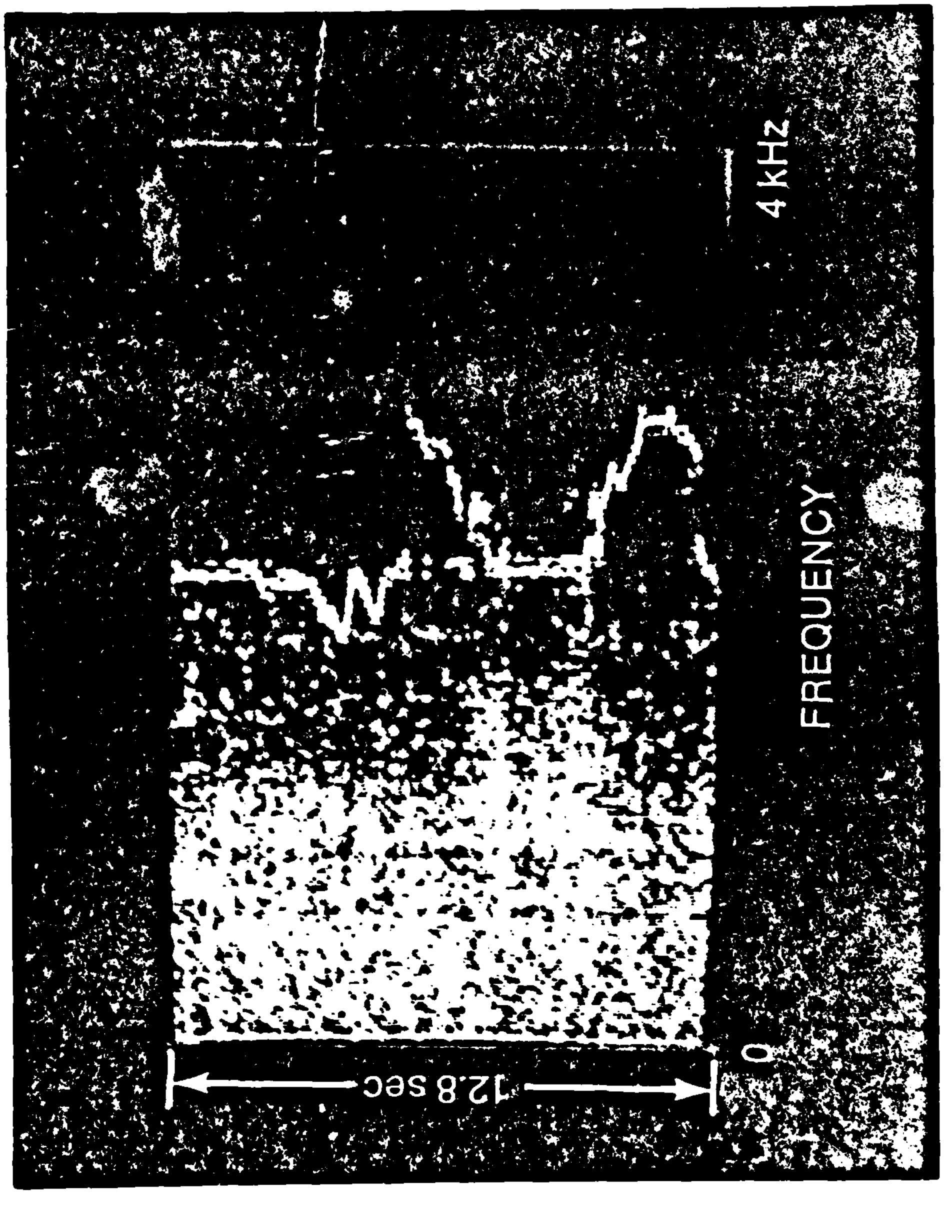

Frequency Domain Dynamics

Slide 9

Another data set of approximately 45 minutes in duration was analyzed by listening to its aural character, while visually observing its frequency-time spectrum. The slide shows a 12.8 second portion. At about 2 kHz, we clearly observe a dynamic tonal that sounded like a squeak. To the left, we notice a heavy lightened area that probably corresponds with ice rubbing since this sound was aurally detected in the background at the same time.

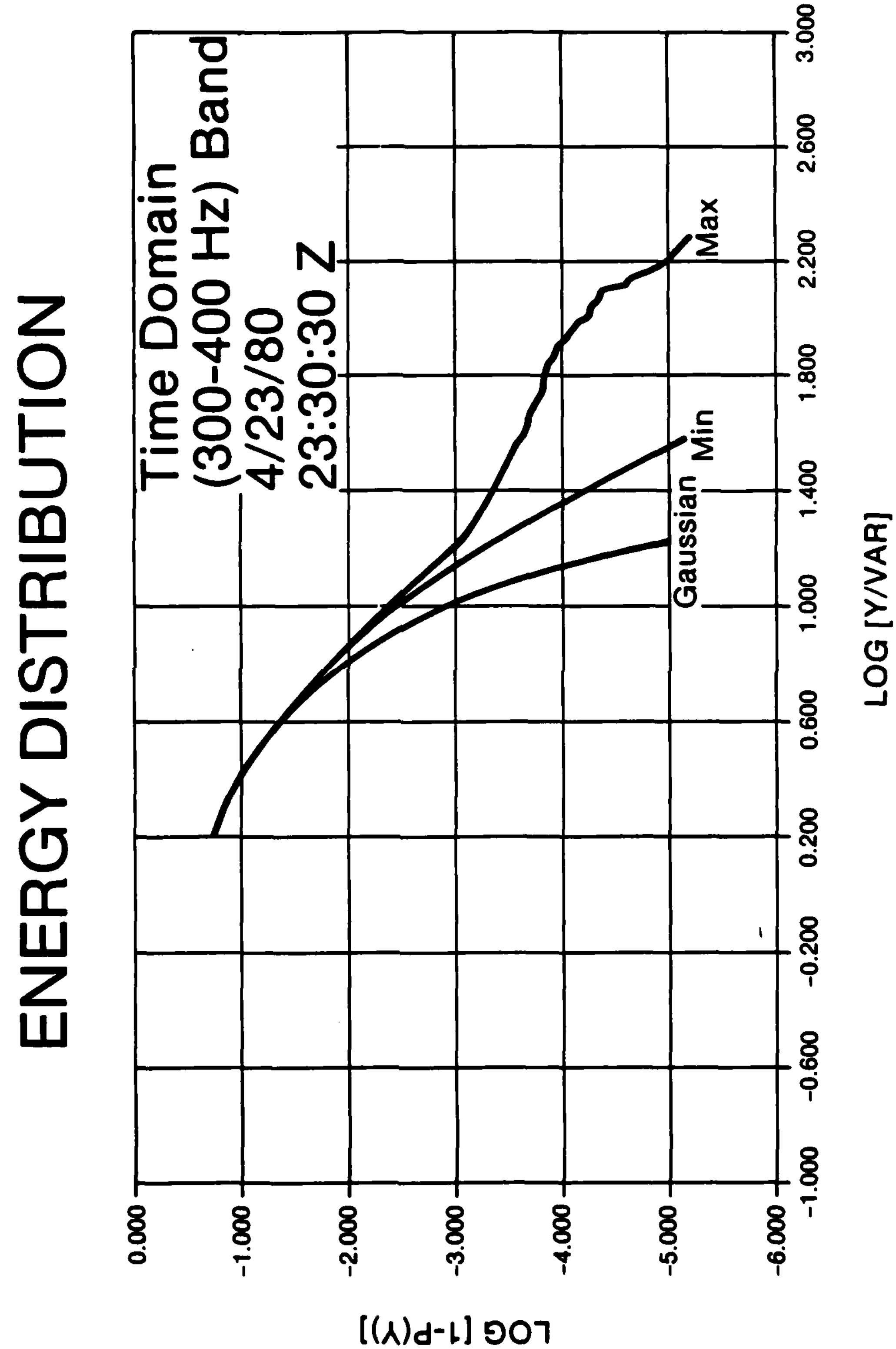
ENERGY DISTRIBUTION
Time Domain
(300-400 Hz) Band
4/23/80
23:30:30 Z
Max
Min
Gaussian
LOG [Y/VAR]
LOG [1-P(Y)]
-1.000
-0.600
-0.200
0.200
0.600
1.000
1.400
1.800
2.200
2.600
3.000
0.000
-1.000
-2.000
-3.000
-4.000
-5.000
-6.000

Slide 10

As we mentioned previously, a 300-400 Hz band was statistically analyzed. The slide shows the time domain energy distribution for this band. The axes are as we previously described them. For this case, we sampled at a 2 kHz rate. The total data segment for the distribution in the slide is 14.5 minutes. We estimated the energy distribution in approximately 2.4-minute intervals, giving 6 estimates in total. Shown in the graph are the energy distributions that deviated (in the tail behavior) least and most from the Gaussian distribution. These curves are indicated on the slide as "Min" and "Max," respectively. The curve marked "Gaussian" represents the case for Gaussian noise at the input to the square-law device.

Statistical Moments for the 300-400 Hz Band

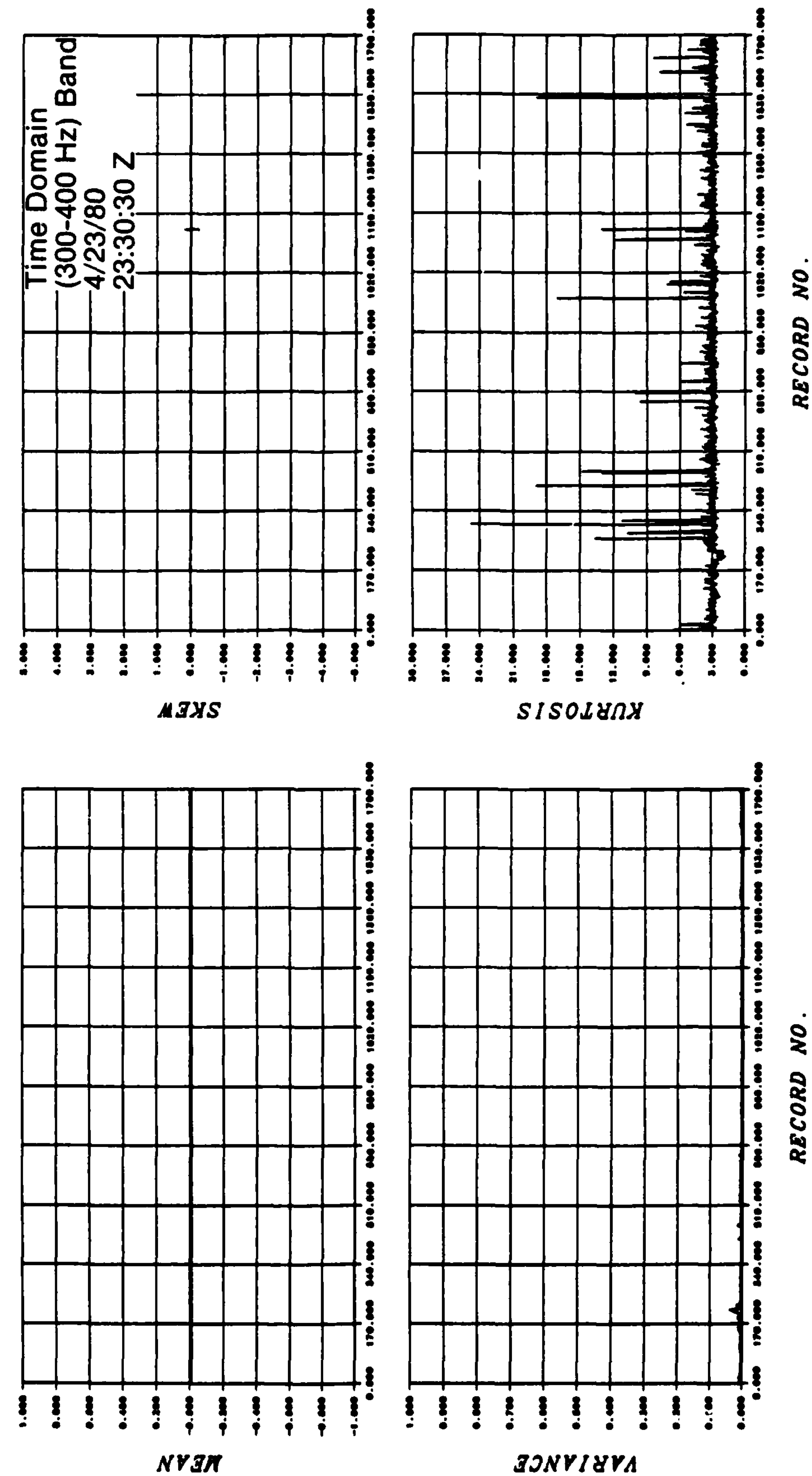

Slide 11

We estimated the mean, variance, skew, and kurtosis at the output of the 300-400 Hz band. The sampling rate was 2 kHz so each 1024 sample record represents 0.512 second. The total data time interval was, therefore, approximately 14.5 minutes. The mean and skew are now zero for practically the whole data length. Note that the variance is diminished from the full band case, which is to be expected; however, its variability is small. As we mentioned previously, the variability for the most part was caused by energy from the higher frequency bands. On the other hand, we obtained the significant result that many of the records deviated from the Gaussian assumption based on the kurtosis.

Frequency Domain Statistics

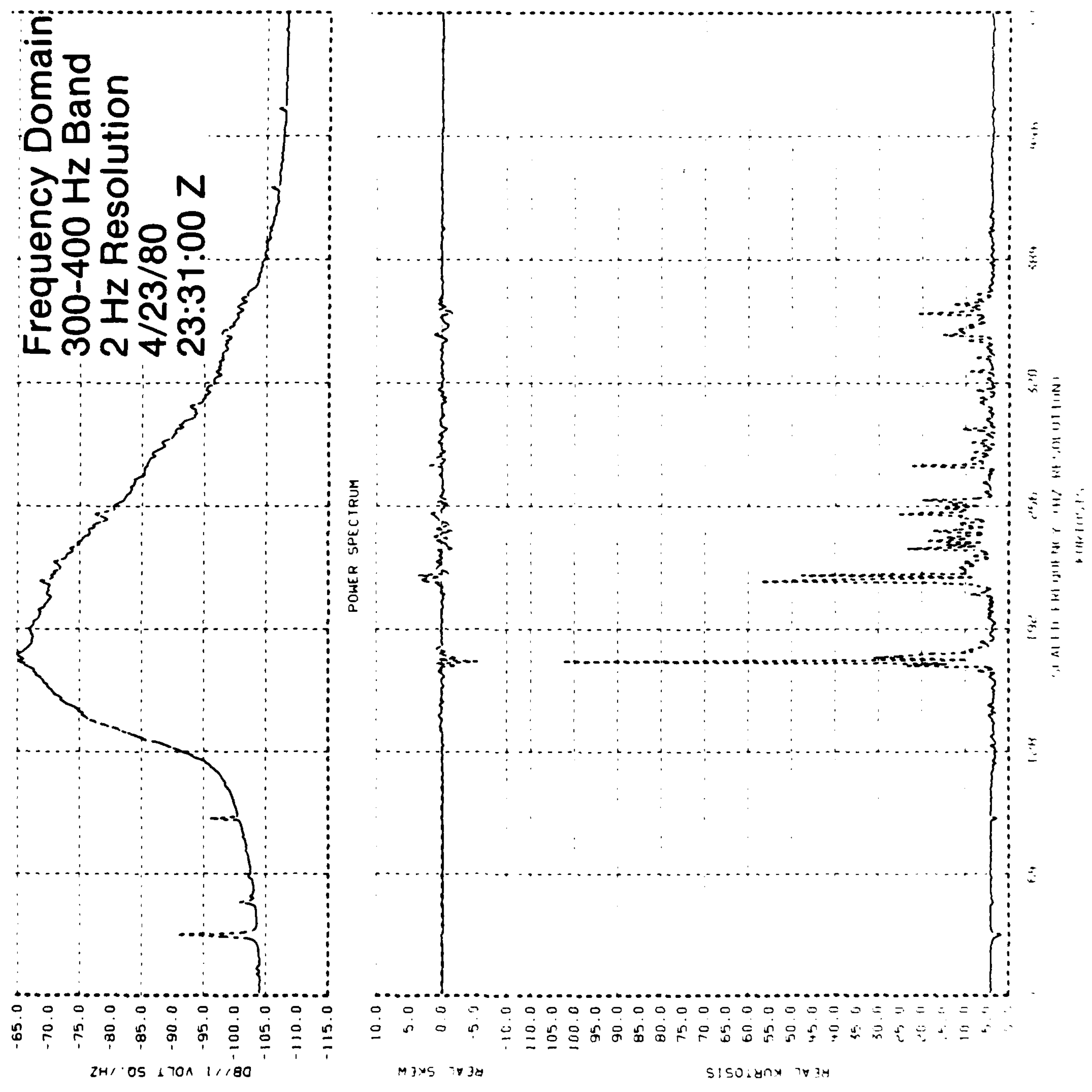

Slide 12

The data at the output of the 300-400 Hz band were sampled at a 2-kHz rate and FFT'd using a 1024 point FFT. This procedure gave a resolution of 2 Hz. A total of 750 consecutive FFT's were processed for an overall time interval of 6.25 minutes. The averaged power spectrum for the 750 consecutive FFT's is shown on the top graph of the slide. We also estimated the skew and kurtosis for both the real and imaginary parts over the full 750 consecutive FFT's. Only the real parts are shown in the figures. Similar, but not identical, results were obtained for the imaginary parts for both the skew and kurtosis.

Note the 60-Hz tonal in the power spectrum, which is due to an electrical ground loop. The corresponding kurtosis (indicated in the bottom graph by a dip in the plot at 60 Hz) is about 1.8. The next dips at higher frequencies are due to harmonics of the 60 Hz ground loop. These dips are much less pronounced (approximately 2.6 and 2.2, respectively) compared with the 60 Hz dip indicating that kurtosis is signal-to-noise ratio dependent. In the 300-400 Hz band, which is clearly seen in the top graph, we find that for many bins both skew and kurtosis deviated from the Gaussian assumption.

FREQUENCY DOMAIN: AMPLITUDE DISTRIBUTION

Data (4/23/80)
BAND (300-400) Hz
23:31:00 Z

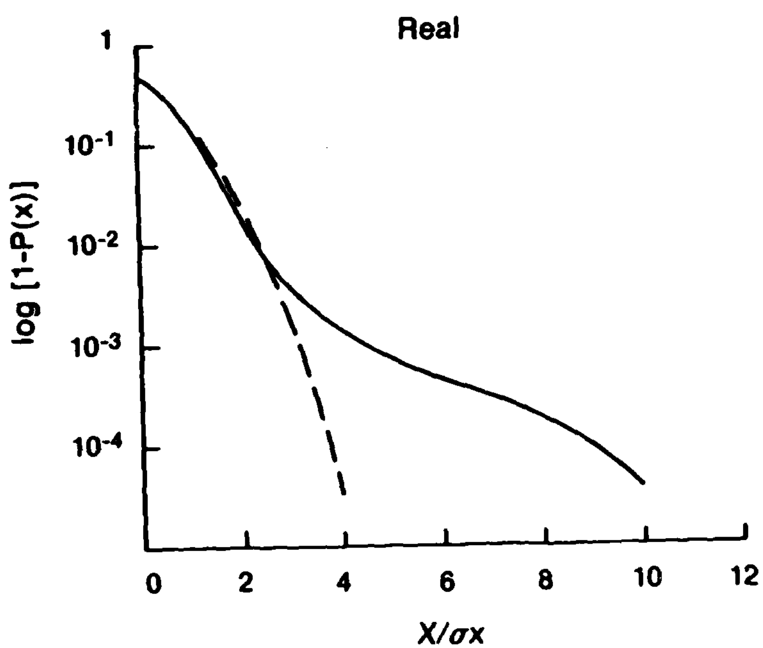

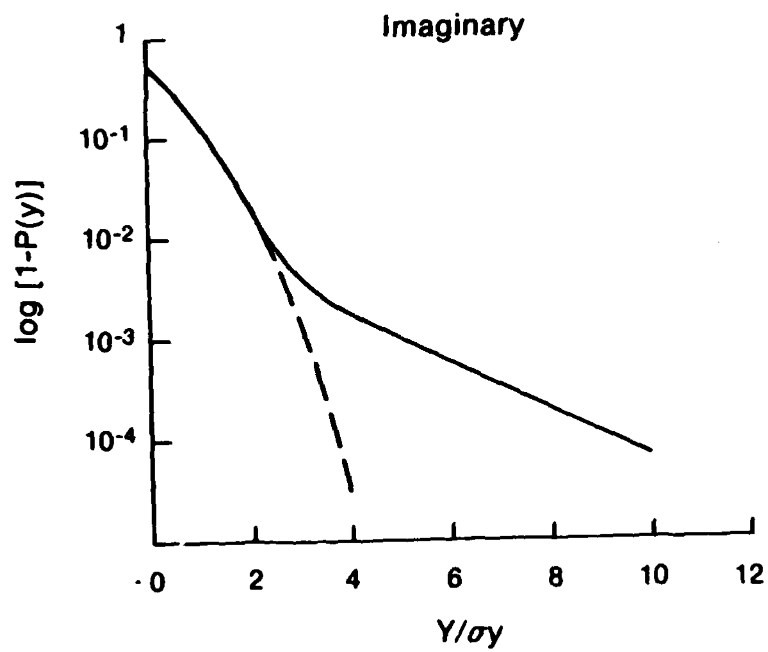

Slide 13

For a small portion of the band, as shown in the previous slide, we estimated the amplitude cdf using the 750 consecutive FFT outputs for both the real and imaginary parts. The end points of the band segment, which extended for 36 bins, was within 1 dB. The total number of bin samples for both the real and imaginary parts, used in the amplitude cdf estimates, were 27,000. The graphs of the real and imaginary amplitude cdf estimates show significant deviation in the tails, compared with the Gaussian amplitude cdf estimates indicated by the dashed curves.

Summary

• Under ice ambient noise in the time domain is, at times, impulsive and highly non-Gaussian.

• Nonstationary variance estimates measured in the full band appear to be due to the energy in the high frequency bands.

• The estimated energy cdf of FRAM II data in the time domain predicted detection thresholds at the .0001 level of 3-10 dB higher than what would be expected for purely Gaussian phenomena.

• Complex skew, kurtosis, and cdf estimates indicate existence of strong non-Gaussian noise in the frequency domain.

Slide 14

In summary, we have shown that under-ice ambient noise in the time domain is at times impulsive and highly non-Gaussian. This finding is consistent with the work of Milne and others.

The non-stationary variance estimates, measured in the full 2,500 Hz band, appear to be due to the high frequency ice dynamics.

The estimated energy cdf of FRAM II data in the time domain for the full band predicted detection thresholds at the 0.0001 level of 3 to 10 dB higher than what would be expected for purely Gaussian phenomena.

These new findings, based on the complex skew, kurtosis, and cdf estimates, indicate the existence of strong non-Gaussian noise in the frequency domain.

Initial Distribution List

ADDRESSEE	NO. OF COPIES
ONR (Dr. E. J. Wegman, ONR-430)	1
NAVSEASYSCOM (CDR R. Welsh, Code 63D; Dr. D. Porter, Code 63R-11)	2
NCSC (E. Moritz, Code 791)	1
Princeton University (Dr. S. C. Schwartz)	1
University of Rhode Island (Dr. D. Tufts)	1
Analysis & Technology, Inc. (Dr. Philip L. Stocklin)	1
Indian Institute of Technology (A. L. Vyas, R. Bahl)	2
ARL University of Texas (Dr. Marshall Frazer, Dr. C. S. Penrod, G. Wilson)	3
MIT (I. Dyer, A. Baggeroer)	1
DTIC	12